Copyright © 1991 by ASME

Active Control of Rotating Stall in a Low Speed Axial Compressor

J. PADUANO, A. H. EPSTEIN, L. VALAVANI, J. P. LONGLEY*, E. M. GREITZER, G. R. GUENETTE
Gas Turbine Laboratory
Massachusetts Institute of Technology
Cambridge, MA 02139

ABSTRACT

The onset of rotating stall has been delayed in a low speed, single-stage, axial research compressor using active feedback control. Control was implemented using a circumferential array of hot wires to sense rotating waves of axial velocity upstream of the compressor. Circumferentially travelling waves were then generated with appropriate phase and amplitude by "wiggling" inlet guide vanes driven by individual actuators. The control scheme considered the wave pattern in terms of the individual spatial Fourier components. A simple proportional control law was implemented for each harmonic. Control of the first spatial harmonic yielded an 11% decrease in the stalling mass flow, while control of the first and second harmonics together reduced the stalling mass flow by 20%. The control system was also used to measure the sine wave response of the compressor, which behaved as would be expected for a second order system.

NOMENCLATURE

C_n	complex spatial Fourier coefficient (Eq. (5))
IGV	inlet guide vane
n	mode number
P	static pressure
P_T	total pressure
R_n	controller gain ($R_n = |Z_n|$)
r	mean compressor radius
$\tilde{t}$	non-dimensional time ($= Ut/r$)
U	mean compressor blade speed
V_k	axial velocity measurement (Eq. (5))
Z_n	controller complex gain and phase
β_n	controller phase for n'th mode ($\beta_n = |Z_n|$)
γ	IGV stagger angle
$\delta( )$	perturbed quantity
θ	circumferential coordinate
λ	rotor inertia parameter
μ	rotor + stator inertia parameter

μ_{IGV}	IGV inertia parameter
ρ	density
ϕ	local flow coefficient (axial velocity/U)
$\bar{\phi}$	area averaged flow coefficient
ψ	compressor pressure rise $(P-P_T) / (\rho U^2)$

Subscripts

n	n'th circumferential Fourier mode
R	real part of complex quantity
I	imaginary part of complex quantity

INTRODUCTION

Axial compressors are subject to two distinct aerodynamic instabilities, rotating stall and surge, which can severely limit compressor performance. Rotating stall is characterized by a wave travelling about the circumference of the machine, surge by a basically one-dimensional fluctuation in mass flow through the machine. Whether these phenomena are viewed as distinct (rotating stall is local to the blade rows and dependent only on the compressor, while surge involves the entire pumping system -- compressor, ducting, plenums, and throttle) or as related (both are natural modes of the compression system with surge corresponding to the zeroth order mode), they generally cannot be tolerated during compressor operation. Both rotating stall and surge reduce the pressure rise in the machine, cause rapid heating of the blades, and can induce severe mechanical distress.

The traditional approach to the problem of compressor flow field instabilities has been to incorporate various features in the aerodynamic design of the compressor to increase the stable operating range. Balanced stage loading and casing treatment are examples of design features that fall into this category. More recently, techniques have been developed that are based on moving the operating point close to the surge line when surge does not threaten, and then quickly increasing the margin when required, either in an open or closed loop manner. The open loop techniques are based on observation, supported by many years of experience, that compressor stability is strongly influenced by inlet distortions and by pressure transients caused by augmentor ignition and, in turn, that inlet distortion can be correlated with aircraft angle of attack and yaw angle. Thus, significant gains have been realized by coupling

---

* Current Address: Whittle Laboratory, Cambridge University, Cambridge, England

the aircraft flight control and engine fuel control so that engine operating point is continually adjusted to yield the minimum stall margin required at each instantaneous flight condition (Yonke et al., 1987).

Closed loop stall avoidance has also been investigated. In these studies, sensors in the compressor were used to determine the onset of rotating stall by measuring the level of unsteadiness. When stall onset was detected, the control system moved the operating point to higher mass flow, away from the stall line (Ludwig and Nenni, 1980). While showing some effectiveness at low operating speeds, this effort was constrained by limited warning time from the sensors and limited control authority available to move the compressor operating point.

This paper presents the initial results of an alternative and fundamentally different means for attacking the problem posed by rotating stall. Here, we *increase* the stable flow range of an axial compressor by using closed loop control to damp the unsteady perturbations which lead to rotating stall. In contrast to previous work, this dynamic stabilization concept increases the stable operating range of the compressor by moving the stall point to lower mass flows, as illustrated conceptually in Fig. 1. There appear to be at least two advantages of this new technique. One is that engine power always remains high with dynamic stabilization while power must be cut back with stall avoidance (often at critical points in the flight envelope). A second advantage is that the gain in operating range can be potentially greater. In the following sections, we briefly describe those elements in the theory of compressor stability that are relevant to active stability enhancement, discuss the design of the experimental apparatus, and present the experimental results.

Conceptual View of Compressor Stability and Active Stall Control

We consider rotating stall to be one of the class of natural instabilities of the compression system, as analyzed for example by Moore and Greitzer (1986) for low-speed machines of high hub-to-tip radius ratio. Their model predicts that the stability of the compressor is tied to the growth of an (initially small amplitude) wave of axial velocity which travels about the circumference of the
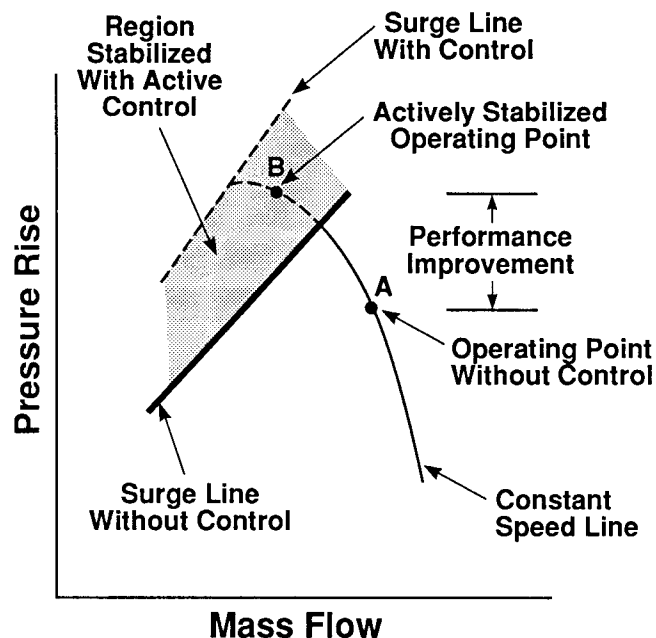
compressor. If the wave decays (i.e. its damping is greater than zero), then the flow in the compressor is stable. If the wave grows (wave damping negative), the flow in the compressor is unstable. Thus, wave growth and compressor flow stability are equivalent in this view.

One prediction of this model that is useful for present purposes is that rotating waves should be present at low amplitude prior to stall. McDougall (1988, 1989) has identified these waves in a low speed, single-stage compressor, and Garnier, et al (1990) observed them in both a single and a three-stage low speed compressor, and in a three-stage high speed compressor. The waves were often evident long (ten to one hundred rotor revolutions) before stall. It was found that the waves grew smoothly into rotating stall, without large discontinuities in phase or amplitude, and that the wave growth rate agreed with the theory of Moore and Greitzer (1986). Further, the measurements showed how the wave damping, and thus the instantaneous compressor stability, could be extracted from real time measurements of the rotating waves.

In 1989, Epstein, Ffowcs Williams, and Greitzer suggested that active control could be used to artificially damp these rotating waves when at low amplitude. If, as the theory implies, rotating stall can be viewed as the mature form of the rotating disturbance, damping of the waves would prevent rotating stall from developing, thus moving the point of instability onset as in Fig. 1. It was proposed that the compressor stability could be augmented by creating a travelling disturbance with phase and amplitude based on real time measurement of the incipient instability waves. This paper presents an experimental investigation of this idea.

The basic concept is to measure the wave pattern in a compressor and generate a circumferentially propagating disturbance based on those measurements so as to damp the growth of the naturally occurring waves. In the particular implementation described herein, shown schematically in Fig. 2, individual vanes in an upstream blade row are "wiggled" to create the travelling wave velocity disturbance. The flow which the upstream sensors and the downstream blade rows see is a combination of both the naturally occurring instability waves and the imposed control disturbances. As such, the combination of compressor and controller is a different machine than the original compressor - with different dynamic behavior and different stability.

At this point, it is appropriate to present the rotating stall model and connect it with the idea of control. Here, it is the structure of the model that is most important rather than the fluid mechanic details. Since the structure provides a framework for design of the control system, the quantitative details can be derived by fitting experimental data to the model.

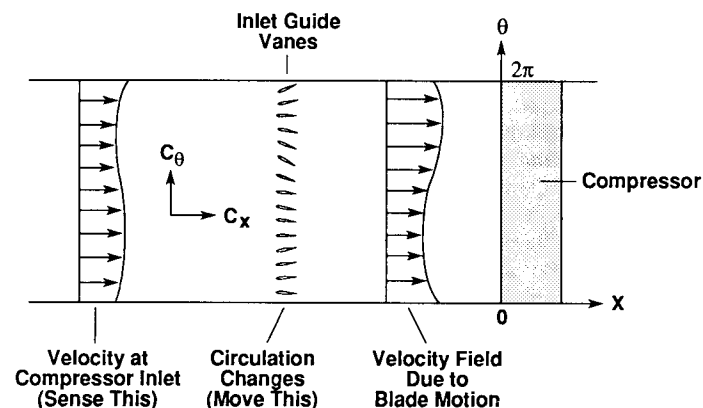The existing models for rotating stall inception in multi-row

Fig. 1: The intent of active compressor stabilization is to move the surge line to lower mass flow

Fig. 2: Conceptual control scheme using "wiggly" inlet guide vanes to generate circumferential travelling waves

2

axial compressors are typified by an equation for the velocity and pressure perturbations of the form

$$\frac{\delta P_{compressor}^{exit} - \delta P_{T_{compressor}}^{inlet}}{\rho U^2} = \left(\frac{d\psi}{d\phi}\right)\delta\phi - \lambda\frac{\partial\delta\phi}{\partial\theta} - \mu\frac{\partial\delta\phi}{\partial\tilde{t}} \qquad (1)$$

Here, δP and δP_T are the static and total pressure perturbations respectively, $\delta\phi$ is the non-dimensional axial velocity perturbation, λ and μ are non-dimensional parameters reflecting the fluid inertia in stator and rotor passages respectively, $(d\psi/d\phi)$ is the slope of the non-dimensional compressor characteristic, and $\tilde{t}$ is a non-dimensional time, $\tilde{t} = tU/r$. Equation (1) has been shown in several publications (e.g. Hynes and Greitzer, 1987; Longley, 1988) and we will not present its development here. The equation is an expression of the matching conditions (across the compressor) for flowfields upstream and downstream of the compressor and, as such, upstream and downstream flow field descriptions are needed to be able to find a solution.

Using these, Longley (1990) has shown that one can put Eq. (1) in a wave operator form. For the nth spatial Fourier coefficient, this is

$$\left\{\left(\frac{2}{|n|}+\mu\right)\frac{\partial}{\partial\tilde{t}} + \lambda\frac{\partial}{\partial\theta}\right\}\delta\phi = \left(\frac{d\psi}{d\phi}\right)\delta\phi \qquad (2)$$

The left-hand side of Eq. (2) is a convective operator corresponding to circumferential propagation with velocity $\lambda/(2/(|n|+\mu)) \cdot$ (rotor speed). In addition, the growth rate of the wave is dependent on the slope of the compressor characteristic. If $(d\psi/d\phi)$ is positive the waves grow; if negative they decay. Neutral stability (wave travelling with constant amplitude) occurs at $(d\psi/d\phi) = 0$.

We can cast Eq. (2) in a form that is more useful for control by considering a purely propagating disturbance. The first Fourier mode will be of the form $e^{i\theta}$, so Eq. (2) can be written as

$$(2+\mu)\frac{\partial\delta\phi}{\partial\tilde{t}} + \left[i\lambda - \left(\frac{d\psi}{d\phi}\right)\right]\delta\phi = 0 \qquad (3)$$

Thus far, the equations presented have been for flow associated with uncontrolled compressor dynamics. If, in addition, we model the control as due to perturbations in IGV stagger, $\delta\gamma$, we obtain the following equation for the first Fourier mode:

$$(2+\mu)\frac{\partial\delta\phi}{\partial\tilde{t}} + \left[i\lambda - \left(\frac{\partial\psi}{\partial\phi}\right)\right]\delta\phi + \left[i\overline{\phi}\mu_{IGV}\left(\frac{\partial\psi}{\partial\phi}\right) - \left(\frac{\partial\psi}{\partial\gamma} - \overline{\phi}\mu_{IGV}\,\lambda\right)\right]\delta\gamma$$

$$- i\overline{\phi}\mu_{IGV}\left(1 + \mu - \frac{\mu_{IGV}}{2}\right)\frac{\partial\delta\gamma}{\partial\tilde{t}} = 0 \qquad (4)$$

where $\overline{\phi}$ is the axisymmetric (annulus averaged) flow coefficient, μ_{IGV} is the fluid inertia parameter for the IGV's, and $(\partial\psi/\partial\gamma)$ represents the incremental pressure rise obtainable from a change in IGV stagger, γ.

This is formally a first order equation for $\delta\phi$, however it must be remembered that the quantity of interest is the real part of $\delta\phi$. If we express $\delta\phi$ in terms of its real and imaginary parts, $\delta\phi = \delta\phi_R + i\delta\phi_I$, then Eq. (4), which is a coupled pair of first order equations for $\delta\phi_R$ and $i\delta\phi_I$, becomes mathematically equivalent to a second order equation for $\delta\phi_R$. The form thus used in the system identification discussed below is thus second order. Another way to state this is that a first order equation with a complex (or pure imaginary) pole is equivalent to a second order system in the appropriate real valued states.

The second order model of compressor behavior is useful for two reasons. First, it can be tested experimentally in a straightforward manner. Second, it provides both a conceptual qualitative framework about which to design a control system (i.e. the stabilization of a second order system) and, given the results of the experimental test, the quantitative inputs required to do the control system design.

EXPERIMENTAL APPARATUS

A 0.52 meter diameter, single-stage low speed research compressor was selected as a test vehicle due to its relative simplicity. The general mechanical construction of the machine was described by Lee and Greitzer (1988), and the geometry of the build studied here is given in Table 1. The apparatus can be considered to consist of four sections: the compressor (described above), instrumentation for wave sensing, actuators for wave launching, and a signal processor (controller). The design of the last three components is discussed below.

TABLE 1
SINGLE-STAGE COMPRESSOR GEOMETRY

Tip Diameter	0.597 m		
Hub-to-Tip Ratio	0.75		
Axial Mach No.	0.10		
Operating Speed	2700 RPM		

	IGV	Rotor	Stator
Mean Line Stagger	0	35°	22.5°
Chamber Angle	0	25°	25°
Solidity	0.6	1	1
Aspect Ratio	0.9	2.0	1.9

The sensors used in the present investigation are eight hot wires evenly spaced about the circumference of the compressor, 0.5 compressor radii upstream of the rotor leading edge. The wires were positioned at midspan and oriented so as to measure axial velocity. Hot wires where chosen because their high sensitivity and frequency response are well suited to low speed compressors. The sensors were positioned relatively far upstream so that the higher harmonic components of the disturbances generated by the compressor would be filtered (the decay rate is like $e^{-n|x|/r}$, where n is the harmonic number). This reduced the likelihood of spatial aliasing of the signal. With eight sensors, the phase and amplitude of the first three disturbance harmonics may be obtained. The outputs of the anemometers were filtered with four pole Bessel filters with a cutoff frequency of 22 times rotor rotation. The axial location of the sensors is important in determining the signal to noise ratio (SNR) of the rotating wave measurements; this question was studied by Garnier et. al. (1990), who showed the SNR to be greatest upstream of the stage.

There are many ways to generate the required travelling waves in an axial compressor. Techniques involving oscillating the inlet guide vanes (IGV's), vanes with oscillating flaps, jet flaps, peripheral arrays of jets or suction ports, tip bleed above the rotor, whirling the entire rotor, and acoustic arrays were all considered on the basis of effectiveness, complexity, cost, and technical risk. For this initial demonstration in a low speed compressor, oscillating the IGV's was chosen on the basis of minimum technical risk.

Considerable care was taken in design of the actuation system to maximize effectiveness and minimize complexity and cost. An unsteady singularity method calculation of the potential flow about a cascade was carried out first to evaluate tradeoffs between blade angle of attack and flow turning angles versus cascade solidity, fraction of the cascade actuated, and airfoil aspect ratio (Silkowski,
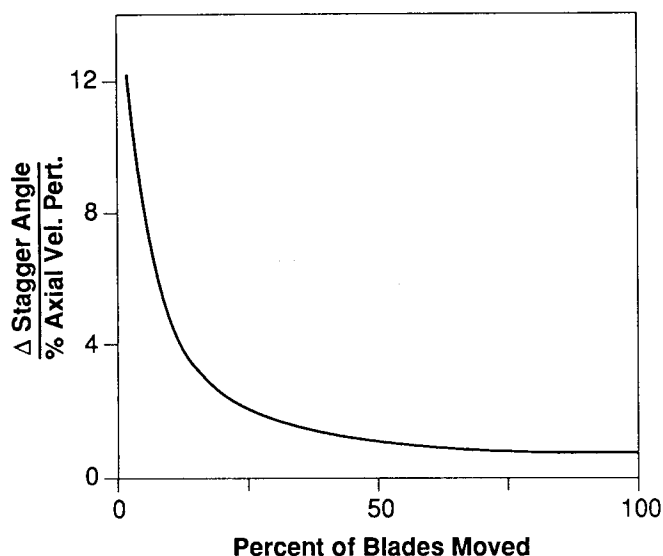
3

Fig. 3: Calculated blade stagger angle change required to generate a given first harmonic axial velocity perturbation as a function of the fraction of the blade row actuated

Fig. 4: Compressor flow path

1990). The unsteady flow was examined since, although the reduced frequency of the IGV airfoil relative to rotating stall is about 0.3 for the first harmonic, several harmonics may be of interest. Calculations were also performed to evaluate the relative effectiveness of bang-bang actuation versus continuous airfoil positioning. As an example of these actuation studies, the tradeoff between the peak airfoil angle of attack excursion and the fraction of the cascade actuated is shown in Fig. 3. As the fraction of the airfoils which is actuated is increased, the angle of attack requirements on individual blades are reduced.

The limits to blade motion are set by both mechanical constraints (i.e., actuator torque limits) and airfoil boundary layer separation at large angles of attack. A NACA 65-0009 airfoil section was chosen due to its good off-angle performance and relatively low moment. The airfoils were cast from low density epoxy to reduce their moment of inertia. A coupled steady inviscid-viscous solution of the flow over the blades indicated that the boundary layers would stay attached at angles of attack up to fifteen degrees (Drela, 1988).

In this experiment, blade actuation torque requirements are set by the airfoil inertia since the aerodynamic forces are small. Both hydraulic and electric actuators are commercially available with sufficient torque and frequency response. Hollow core D.C. servo motors were selected because they were considerably less expensive than the equivalent hydraulic servos. The blades and motors have roughly equal moments of inertia.

For a given IGV solidity, the number of actuators required can be reduced by increasing the blade chord, but this is constrained by actuator torque and geometric packaging. The final IGV design consists of twelve untwisted oscillating airfoils with an aspect ratio of 0.9 and a solidity of 0.6 (Fig. 4). The complete actuation system has a frequency response of 80 Hz (approximately eight times the fundamental rotating stall frequency) at plus or minus ten degrees of airfoil yaw. The flow angle distribution measured at the rotor leading edge station (with the rotor removed) for a stationary ten degree cosine stagger pattern of the IGV's is compared in Fig. 5 to a prediction of the same flow made by Silkowski (1990).

The control law implemented for the tests described here is a simple proportionality; at each instant in time, the nth spatial mode of the IGV stagger angle perturbation is set to be directly proportional to the nth mode of the measured local velocity perturbation. The
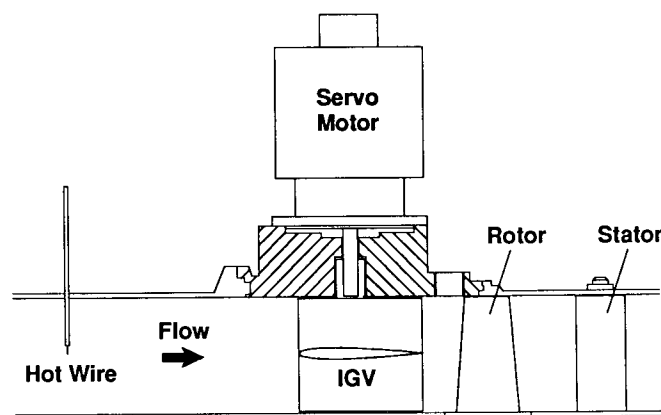
complete control loop consisted of the following steps. First, the sensor signals are digitized. Then, a discrete Fourier transform is taken of the eight sensor readings. The first and/or second discrete Fourier coefficients are then multiplied by the (predetermined) complex feedback gains for that mode. Next, an inverse Fourier transform is taken which converts the modal feedback signals into individual blade commands. These, in turn, are then sent to the individual digital motor controllers. Additional housekeeping is also performed to store information for post-test analysis, limit the motor currents and excursions (for mechanical protection), and correct for any accumulated digital errors.

The controller hardware selection is set by CPU speed requirements (main rotating stall control loop and individual blade position control loops), I/O bandwith (sensor signals in, blade positions out, storage for post-test analysis), operating system overhead, and cost. The final selection was a commercial 20 MHz 80386 PC with co-processor. A multiplexed, twelve bit analog to digital converter digitized the filtered hot wire outputs. The D.C. servo motors were controlled individually by commercial digital motion control boards. Using position feedback from optical encoders on the motors, each motor controller consisted of a digital proportional, integral, derivative (PID) controller operating at 2000 Hz. The entire control loop was run at a 500 Hz repetition rate. Motor power was provided by 350-watt D.C. servo amplifiers. The complete hardware arrangement is shown in Fig. 6.
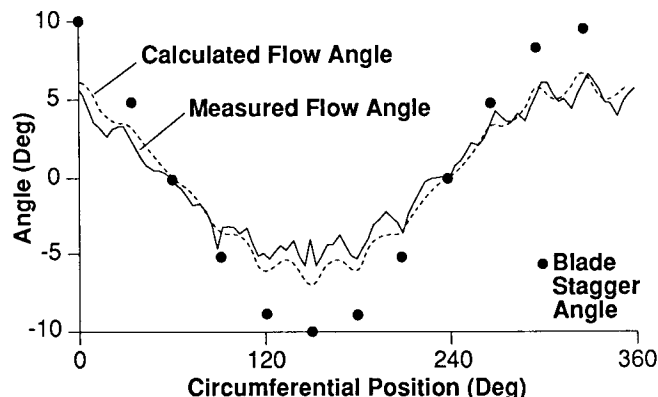

Fig. 5: A comparison of the measured and calculated flow angle generated 0.3 chords downstream by a 10 degree cosine stagger pattern distribution of 12 inlet guide vanes
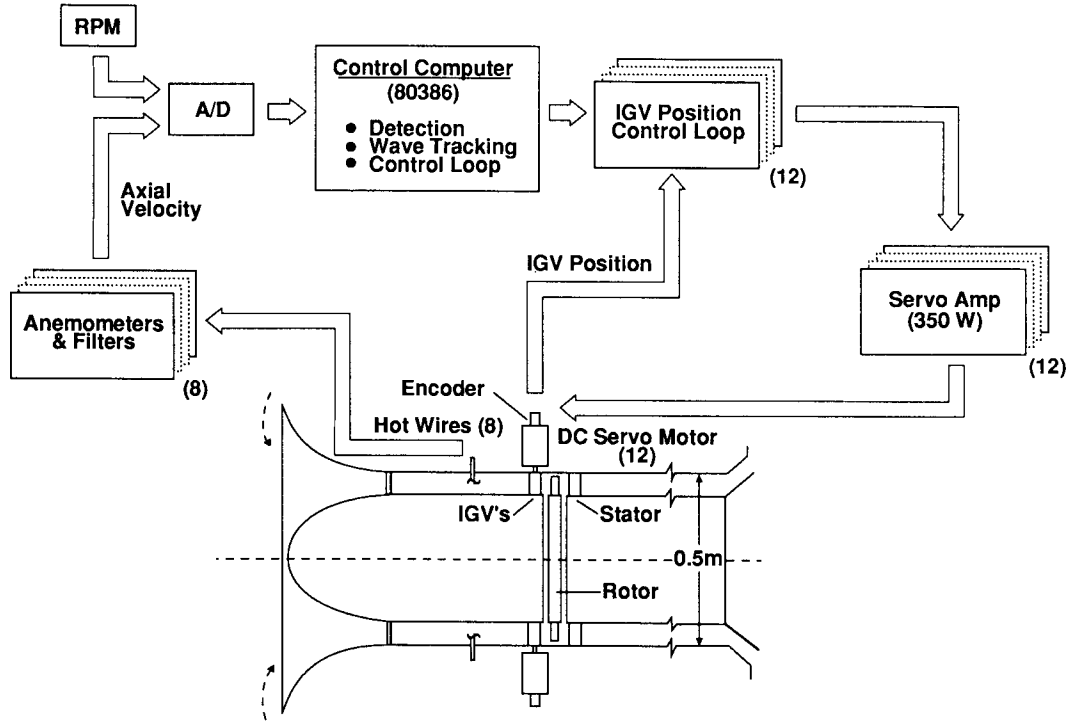
4

Fig. 6: Hardware component of actively stabilized axial flow compressor

OPEN LOOP COMPRESSOR RESPONSE

The inputs and outputs that characterize the fluid system of interest (the compressor and associated flow in the annular region) are the inlet guide vane angles (inputs) and the axial velocity distribution (outputs). In the present configuration this consists of twelve inputs (twelve inlet guide vanes) and eight outputs (eight hot wires) so that the system is multiple input-multiple output. Because the disturbances of interest are of small amplitude, the system behavior can be taken as linear and we can thus express the spatial distribution of the input and output perturbations (or indeed of any other of the flow perturbations) as a sum of spatial Fourier components, each with its own phase velocity and damping. This representation, which is consistent with Eq. (2), allows us to treat the disturbances on a harmonic-by-harmonic basis, and reduces the the input-output relationship to single input-single output terms, an enormous practical simplification.

The complex spatial Fourier coefficient for each mode n is given by

$$C_n = \frac{1}{K} \sum_{k=0}^{K-1} V_k \exp\left[-\frac{2inkπ}{K}\right] \qquad (5)$$

where K is the number of sensors about the circumference (8 in this case), and V_k is the axial velocity measured at angular position k. The magnitude of C_1 is thus the amplitude of the first harmonic at any time and its phase is the instantaneous angular position of the spatial wave Fourier component.

An important concept in the present approach is the connection between rotating stall and travelling wave type of disturbances in the compressor annulus. In this view, the wave damping and the compressor damping are equivalent and determine whether the flow is stable. At the neutral stability point, the damping of disturbances is zero, and close to this point, the damping should be small. (The measurements given by Garnier, et al. (1990) show

this.) Thus, for a compressor operating point near stall, the flow in the annulus should behave like a lightly damped system, i.e., should exhibit a resonance peak when driven by an external disturbance. As with any second order system, the width of the peak is a measure of the damping.

The present apparatus is well suited to establishing the forced response of the compressor since the individual inlet guide vanes can be actuated independently to generate variable frequency travelling waves. The sine wave response of the compressor was measured by rotating the ±10 degree sinusoidal IGV angle distribution shown in Fig. 5 about the circumference at speeds ranging from 0.05 to 1.75 of rotor rotational speed. Figure 7 shows the magnitude of the first spatial Fourier coefficient, as a percentage of the mean flow coefficient, as a function of input wave rotation frequency, i.e. the transfer function for the first spatial mode.

The peak response to the forcing sine wave is seen in Fig. 7 to be at 23% of the rotor rotation frequency. This is close to the frequency observed for the small amplitude waves without forcing (20%) and for the fully developed rotating stall (19%). This behavior supports the view stated previously that the compressor behaves as a second order system.

CLOSED LOOP EXPERIMENTS – ROTATING STALL STABILIZATION OF THE FIRST FOURIER MODE

While the open loop experiments described above are of interest in elucidating the basic structure of the disturbance field in the compressor annulus, this work is principally aimed at suppressing rotating stall using closed loop control. To assess this, experiments were performed using a control scheme of the form

$$[δγ_{IGV}]_{n'th\ mode} = Z_n C_n \qquad (6)$$

where
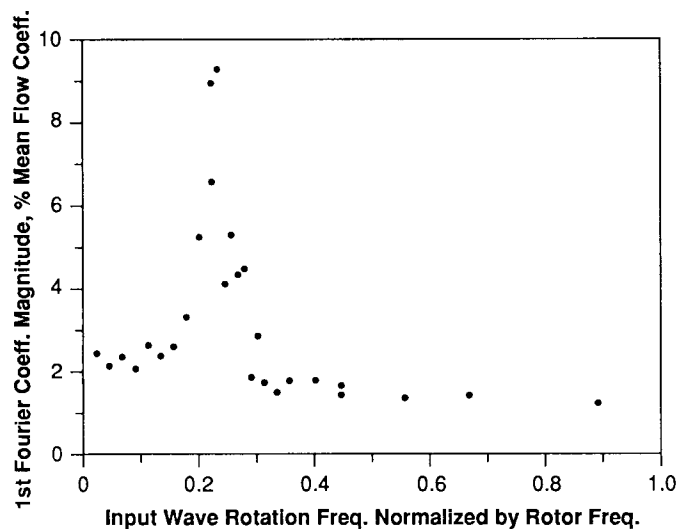
$$Z_n \equiv R_n e^{iβ_n} \qquad (7)$$

5

Fig. 7: Measured open loop response of the first spatial mode of the compressor to a 10° IGV stagger rotating sine wave excitation

In Eqs. (6) and (7), $\delta\gamma_{IGV}$ is the change in inlet guide vane stagger angle. The quantity Z_n is the complex feedback gain for the nth Fourier mode (n'th spatial harmonic component of the disturbance), with R_n the amplitude and β_n the phase angle between the measured axial velocity spatial harmonic (0.5 radii upstream of the rotor) and the input inlet guide vane angular position spatial harmonic. The influence of feedback amplitude (R_n) and phase (β_n) were established with a set of parametric experiments carried on at a flow coefficient (ϕ) close to stall, in a region of marginal flow stability.

Data is shown in Fig. 8 in the form of the power spectral density (PSD) of the first spatial mode axial velocity disturbance (C_1) at two control phase angles (β_1), 0° and 45°. The operating point is fixed at a normally stable flow coefficient of $\phi = 0.475$ (stall without control occurs at $\phi = 0.430$). For each phase, spectra are shown with feedback control and with no control (vanes stationary at zero flow angle). The rotating disturbance is evident in the strong peaks at 23% of rotor rotation frequency. The height of the peaks is a measure of the strength of the rotating waves. The scales are dimensional but all plots are to the same scale so they can be compared directly. The difference between the peak heights with no control in the two cases is due to finite sampling time, i.e., to differences in the ambient disturbance levels during the sampling period.

At 0° phase angle, the peak at 0.23 frequency is higher with active control than with fixed vanes, implying that the feedback control at this phase is amplifying the rotating disturbance waves (i.e. making them less stable). At 45° phase angle, however, the peak with control is lower than that with fixed vanes, implying that control is attentuating the waves in this case. Thus, the ratio of the height of the peak in the PSD with and without control (i.e. the wave amplification) is a measure of the effectiveness of the feedback in influencing the travelling wave's stability. The influence of controller phase (β_1) at fixed gain on the wave amplitude ratio was experimentally evaluated for phase shifts between 0° and 360°, as shown in Fig. 9. For phases between 0° and 150°, the waves are attentuated, while the waves are amplified for phase angles between 160° and 350°. The maximum attenuation found was roughly 30 at $\beta_1 = 75°$, and the maximum amplification of a factor of 1,300 occurs at $\beta_1 = 275°$. Between $\beta_1 = 290$ and $\beta_1 = 345$, the system is unstable (i.e. goes into rotating stall).

If wave stability is equivalent to compressor stability, then compressor stability should be enhanced for control phases at which
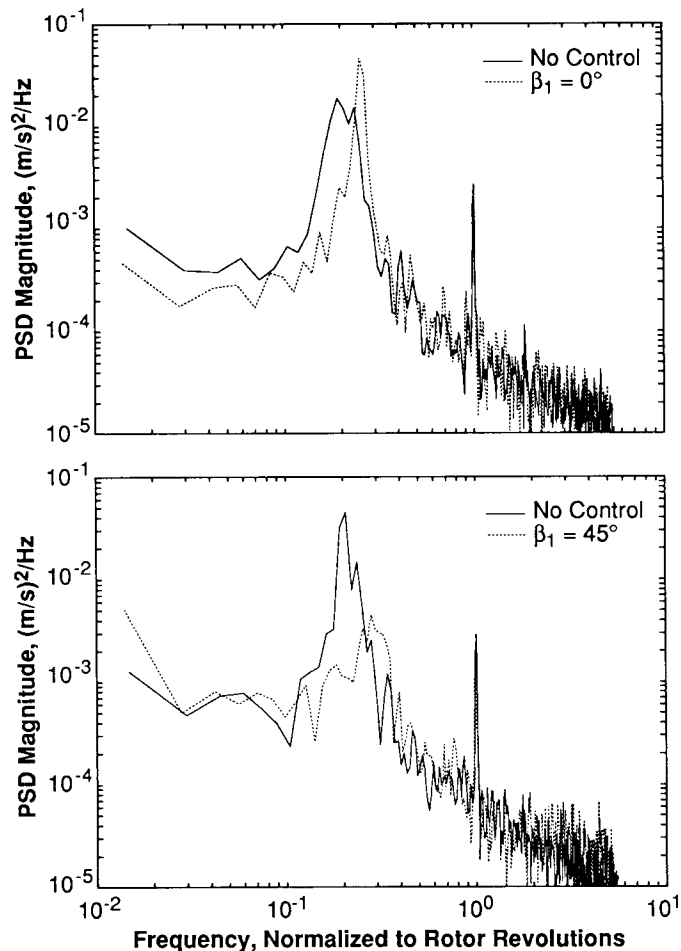

Fig. 8: The influence of proportional feedback control on the power spectral density (PSD) of the first spatial mode of the compressor at two feedback phase angles (β_1) versus the behavior with fixed IGV's
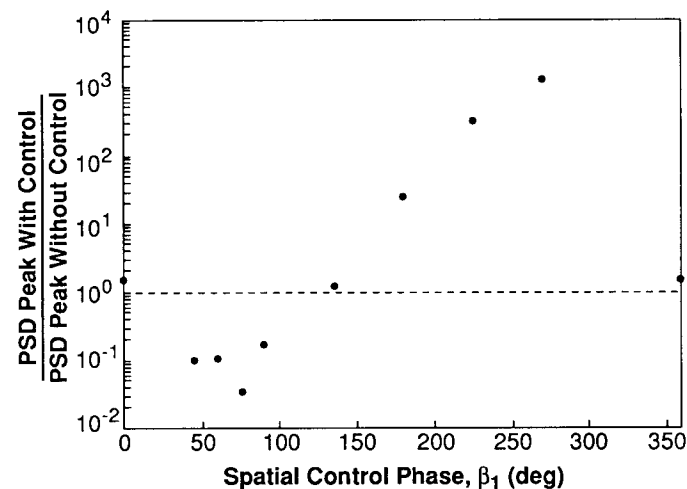

Fig. 9: Influence of feedback control phase angle (β_1) on the strength of the first spatial mode of the flow in the compressor at $\phi = 0.475$
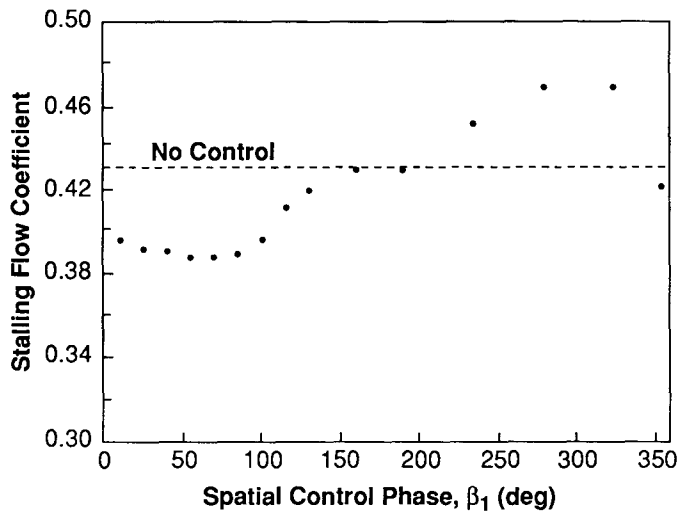
6

Fig. 10: Influence of feedback control phase angle (β_1) on the flow coefficient at which the compressor goes into rotating stall

the waves are attenuated and should be decreased when the waves are amplified. This is indeed the case as illustrated in Fig. 10. Here, the flow coefficient (ϕ) at which the compressor goes into rotating stall as the compressor throttle is very slowly closed ($d\phi/dt = 2\times10^{-5}/$ rotor revolution) is shown as a function of controller phase angle (β_1). Depending upon the phase, the control changes the stalling flow coefficient by as much as $\pm11\%$. Comparison of Figs. 9 and 10 makes clear the connection between wave damping and rotating stall. Rotating stall is suppressed when the waves are damped and is promoted when the waves are amplified.

Figure 11 shows the influence of control of the first spatial harmonic wave in a more familiar form of non-dimensional pressure rise (ψ) versus non-dimensional mass flow (flow coefficient, ϕ) at constant corrected compressor speed. With fixed inlet guide vanes (no control), the compressor stalls at $\phi = 0.43$. With feedback control
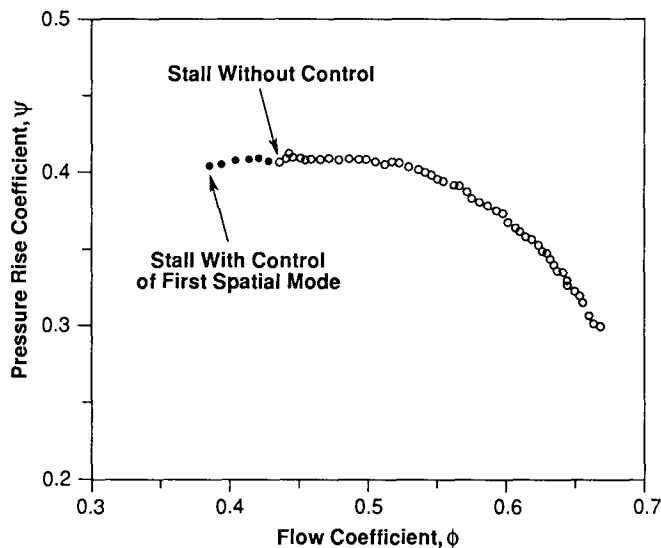

Fig. 11: Non-dimensional pressure rise (ψ) versus mass flow (ϕ) characteristic showing the measured influence of feedback control of the first spatial mode on compressor operating range
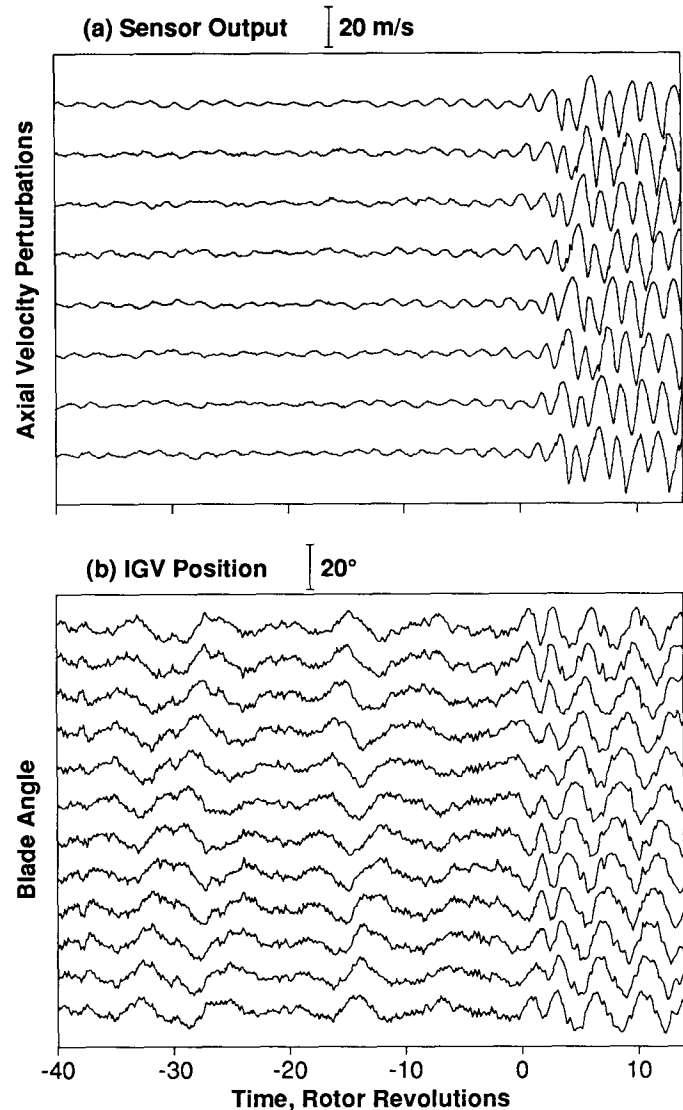

Fig. 12: Time history of compressor sensor output (a) and actuator response (b) with first spatial mode control as the throttle is very slowly closed. Rotating stall onset is at a time of 0.

at the most effective phase found ($\beta_1 = 60°$), the stalling flow coefficient is $\phi = 0.375$, 11% lower. At the phase producing the most wave amplification ($\beta_1 = 275°$), the stalling flow coefficient is 0.475.

Time Resolved System Behavior

Much can be learned from examining the time resolved behavior of the controlled compressor as the throttle is very slowly closed at a controller phase (β_1) of 60°. The overall system behavior is shown in Fig. 12. Here, the onset of stall occurs at a non-dimensional time of 0. Prior to that time, the sensor output is small relative to the rotating stall amplitude. The actuators, however, are clearly producing a travelling wave. (The actuator response to the rotating stall after stall onset is due to the light damping of the blade servos.)

The time evolution measured by a single sensor is shown in Fig. 13. For this compressor with no control (Fig. 13a), the rotating stall grows quite slowly. With control of the first spatial mode (Fig. 13b), the growth is much faster. (Note that this occurs at a lower
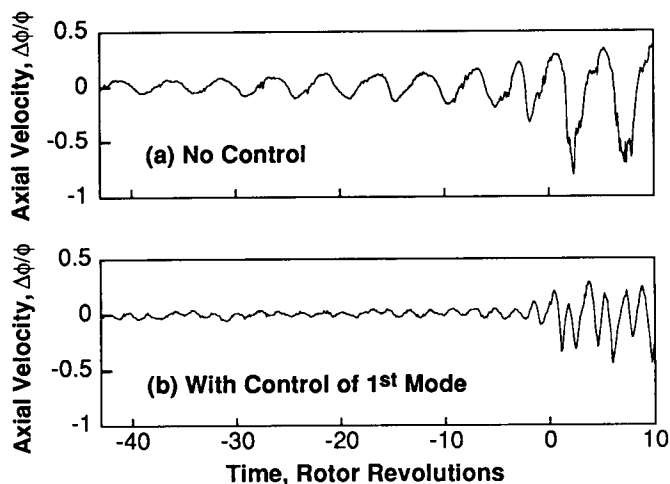
7

Fig. 13: The influence of control on the time history of a single sensor as the throttle is slowly closed to stall the compressor

Fig. 15: Same as Fig. 14, but with control of the first spatial mode

flow coefficient than Fig. 13a.) Further, the disturbances with control have twice the frequency as in the no control case. This is due to the primary disturbance now being a two-cell rotating stall, i.e. the second spatial mode.

The influence of first mode control on the disturbance modal structure is illustrated in Figs. 14 and 15, which show disturbance phase and amplitude versus time. A linear variation of phase with time indicates that the disturbance is propagating at constant speed. Without control (Fig. 14), both the first and second spatial modes are evident in both magnitude and phase for 40 rotor revolutions before stall. The first mode is clearly the strongest everywhere and the fully developed stall is an admixture of both modes. When the first spatial mode is controlled (Fig. 15), it is the second which is stronger prior to stall, and predominates in the fully developed rotating stall.

Control of the Second Spatial Mode

Since the second spatial mode appears predominant when the first mode is under control, it makes sense to control the second mode as well. The effect of simultaneous control of the first two spatial
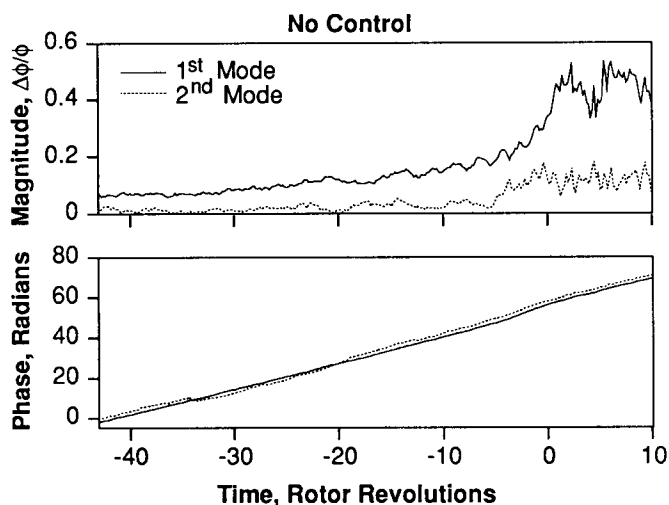
modes on compressor stalling pressure rise is shown in Fig. 16. With both modes under the control, the compressor does not stall until a flow coefficient of $\phi = 0.35$, a 20% increase in operating range over the no control case. Examination of the time behavior of the Fourier coefficients, as the compressor throttle is slowly closed (Fig. 17), shows that, prior to stall, the first and second modes are of about equal strength. At the stall point, the second mode growth is initially more rapid but fully developed stall is predominantly the first mode. This suggests that (nonlinear) mode coupling is important as the wave matures. The measured third spatial mode is relatively weak.

SYSTEM IDENTIFICATION

The measurements presented have been for a compressor with a simple proportional control law, one whose rationale is based on a linear theory as summarized by Eq. (4). There are many analytical tools now available to design more sophisticated control schemes with, hopefully, improved performance. The success of the

Fig. 14: Time history without control of the first two Fourier coefficients as the throttle is slowly closed to stall the compressor at t = 0 revs
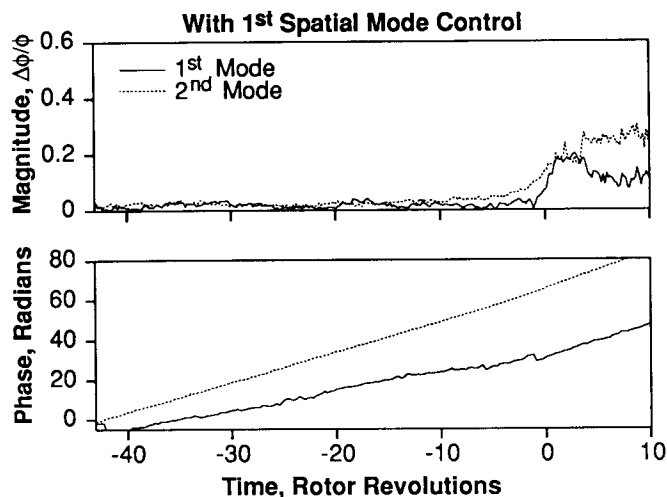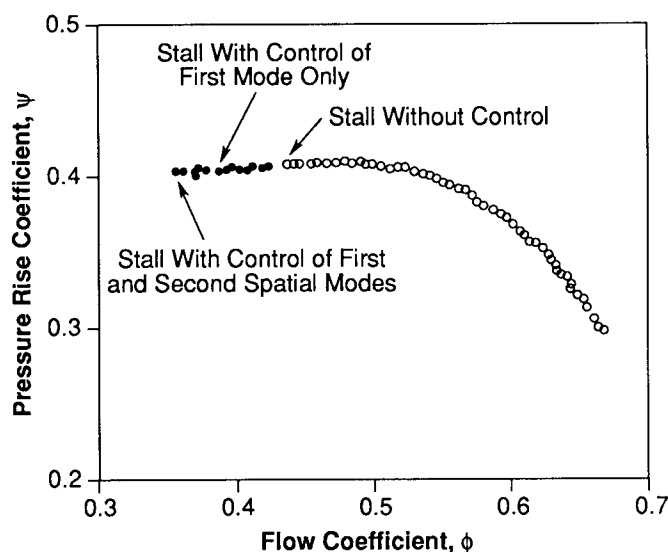

Fig. 16: Compressor characteristic as in Fig. 11, but with active control of first and second spatial modes

8

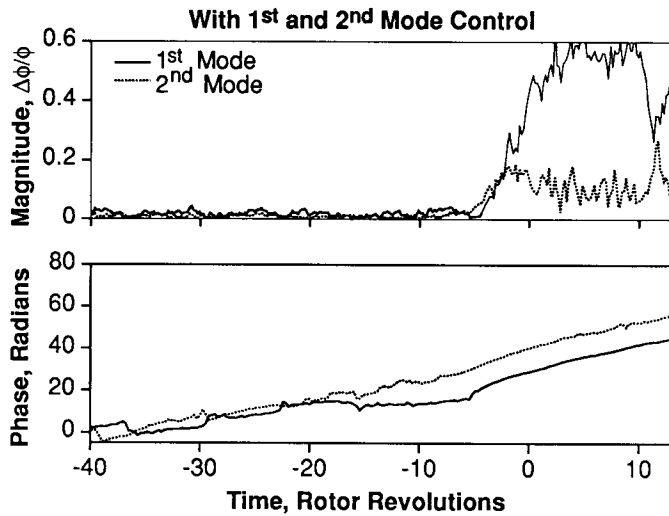Fig. 17: Same as Figs. 14 and 15, but with control of the first and second spatial modes

Fig. 18: Bode plot showing response of the compressor to a sine wave forcing excitation at $\phi = 0.475$

control design, however, will be based in no small part on the fidelity of the system model assumed for the compressor. Also, we are interested in understanding more about the compressor fluid mechanics. The apparatus assembled for the active control experiment is well suited to quantitatively establishing the dynamic response of the compressor by directly measuring its transfer function.

The magnitude behavior of the compressor response to IGV motion was given in Fig. 7. This behavior can be put into a more complete form, and compared to at least the structure of the fluid dynamic model, by plotting the phase and magnitude (Bode diagram) of the transfer function between the first Fourier coefficient of IGV motion and the first Fourier coefficient of the resulting axial velocity perturbations. This transfer function has both a magnitude and a phase, which results from both spatial and time lags between the input and output. We expect the behavior of this system based on the modelling described earlier to be that of a second order system. This should be easily identifiable from experiments such as a rotating sine wave response, for example.

We can express the fluid model of Eq. (4) in more convenient transfer function form as

$$\frac{\delta \phi}{\delta \gamma}(s) = K \frac{s + (A + Bi)}{s + (C + Di)} \tag{8}$$

where s is the Laplace transform variable. The complex form of this transfer function gives rise to second-order behavior in the measured variables, as mentioned previously. The advantage of this form is that it uses the minimum number of parameters to completely specify the transfer characteristics of the system. A linear regression type fit (Lamaire, 1987) can be done for the parameters K, A, B, C, and D. This gives rise to the results shown in Fig. 18, where it can be seen that the response characteristics in the experiment are mimicked by the model. We have obtained this type of fit using various types of IGV inputs: rotating waves, stationary waves with oscillating amplitudes, and stationary waves with random amplitudes. As would be expected in a linear system, the input-output behavior is unaffected by such variations in the character of the input. More details on this system identification can be found in Paduano et al. (1990). Overall, the fit of the second order model to the measurements is very good.

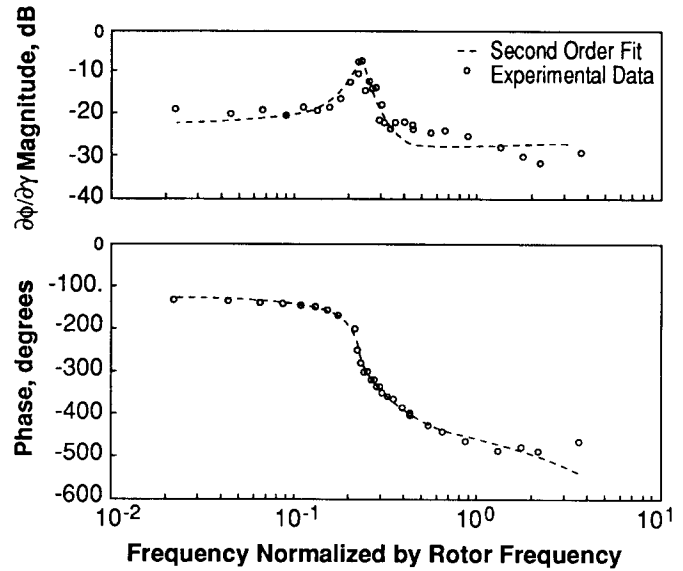In summary, the fidelity of the model fit to the data in Fig. 18

indicates that structure of the fluid model of Eq. (4) is appropriate for this compressor at the flow conditions examined. We have yet to make the quantitative prediction of the Bode plot from the compressor geometry.

DISCUSSION

The most important point of this paper is that these experiments demonstrate that it is physically possible to actively control rotating stall in an axial flow compressor and, by doing so, obtain a useful extension in compressor operating range. A second point is that these experiments more firmly establish a clear link between low amplitude circumferentially propagating disturbances prior to stall and fully developed rotating stall -- when the disturbances are suppressed, rotating stall is prevented. This initial attempt to control rotating stall is encouraging. As is often the case, however, these results raise many more questions than they answer. These questions thus suggest future research directions.

The control law used in the experiments reported herein is quite simple. Considerable effort is being spent on the design of more sophisticated, and hopefully more effective, controllers. The controllers can be useful in two ways -- first, in extending compressor performance and, second, in elucidating the details of the dynamic behavior of the compression system.

At the moment, we do not have a quantitative explanation for the experimentally observed limit to control effectiveness on this compressor (i.e. why is there a 20% flow range improvement rather than a 10% or 30% improvement). Preliminary investigations show that, insofar as the linear system analysis exemplified by Eq. (8) is concerned, the bandwidth and actuator authority limits of the current system have not yet been reached. Another possibility is that higher order modes may drive the instability. Measurements to date have not shown that the third spatial mode is strong (the highest mode which can be resolved with the present instrumentation). Various other nonlinearities can be important. Also, at some flow coefficients, the assumptions which underlie the wave model (Eq. (4)) and the actuation scheme chosen may cease to be valid (i.e. two-dimensional flow). Work is ongoing to address these questions.

There are also more general issues raised that go beyond the behavior of this particular compressor. We have no basis on which

9

to quantitatively extrapolate rotating stall control beyond the machine tested. We note, however, that the wave behavior exploited in this control scheme has been observed on other low and high speed compressors by McDougall and Garnier. Thus, we might expect that those machines could be controlled in a similar fashion to a greater or lesser degree. This question can only be addressed in substance by experimental investigation of other builds of this compressor and of other compressors. A second approach is to quantitatively reconcile the system behavior such as observed experimentally in Fig. 18 with a first principles fluid mechanic model related to compressor geometry as exemplified by Eq. (4). This would facilitate more accurate predictions of compressor behavior with control. Work is ongoing in both areas.

Another concern is the generality of the rotating stall model. Certainly such assumptions as two-dimensionality and incompressible flow are of limited applicability. These models can and are being made more elaborate as fidelity with experimental data requires. It is important to emphasize here that the concept of active control of compressor instabilities is not dependent on the accuracy of any particular mathematical model or conceptual view of the flow in a compressor. The model is there to provide a framework about which to design a control system. Any model would do (assuming it was an accurate representation of the fluid mechanics), although certainly some formulations are much more tractable for control design than others.

Actuation schemes are also important since they influence both the effectiveness of control and the complexity and difficulty of implementation. The approach adopted here was chosen mainly on the basis of minimum technical risk. Many other techniques can be considered and each must be quantitatively evaluated in terms of control authority and implementation difficulty for a particular installation. Research efforts in this area may be fruitful.

As a final point, we would like to comment on the interdisciplinary nature of this research. The effort to date has been successful due to the work of both compressor and controls engineers and it has been challenging for both specialties. In the past several years, we have spent considerable time learning how to talk with each other and can report that the effort appears so far to be rewarding.

CONCLUSIONS

Rotating stall in a low speed axial compressor has been suppressed using active feedback control. To date, a 20% gain in compressor mass flow range has been achieved. The measured dynamic behavior of the compressor has followed predictions from a two-dimensional compressor stability model. These results reinforce the view that the compressor stability is equivalent to the stability of low amplitude waves which travel about the machine circumferentially.

This is a progress report on an ongoing effort. The results so far indicate that active control of large scale fluid mechanic instabilities such as rotating stall in axial compressors is very promising. Much work still needs to be done to assess the practical applicability of these results.

ACKNOWLEDGEMENTS

REFERENCES

Drela, M., 1988, Private Communication.

Epstein, A.H., Ffowcs Williams, J.E., Greitzer, E.M., 1989, "Active Suppression of Aerodynamic Instabilities in Turbomachines," *J. of Prop. and Power*, Vol. 5, No. 2, pp. 204-211.

Garnier, V.H., Epstein, A.H., Greitzer, E.M., 1990, "Rotating Stall Anticipation and Initiation in Axial Compressors," ASME Paper 90-GT-156.

Hynes, T.P., Greitzer, E.M., 1987, "A Method for Assessing Effects of Inlet Flow Distortion on Compressor Stability," *ASME J. Turbomachinery*, Vol. 109, pp. 371-379.

Lamaire, R.O., 1987, "Robust Time and Frequency Domain Estimation Methods in Adaptive Control," Ph.D. Thesis, Department of Electrical Engineering and Computer Science, MIT.

Lee, N.K.W., Greitzer, E.M., 1990, "Effects of Endwall Suction and Blowing on Compressor Stability Enhancement," ASME J. Turbomachinery, Vol. 112, pp. 133-144.

Longley, J.P., 1988, "Inlet Distortion and Compressor Stability", Ph.D. Thesis, Cambridge University Engineering Dept., Cambridge, England.

Longley, J.P., 1990, Unpublished MIT Gas Turbine Laboratory Technical Note.

Ludwig, G.R., Nenni, J.P., 1980, "Tests of an Improved Rotating Stall Control System on a J-85 Turbojet Engine," ASME Paper 80-GT-17.

McDougall, N.M., 1988, "Stall Inception in Axial Compressors", PhD Thesis, Cambridge University.

McDougall, N.M., Cumpsty, N.A., Hynes, T.P., 1989, "Stall Inception in Axial Compressors", submitted to 1989 ASME Gas Turbine Conference.

Moore, F.K., Greitzer, E.M., 1986, "A Theory of Post-Stall Transients in Axial Compressors: Part I - Development of the Equations," *ASME J. of Eng. for Gas Turbines and Power*, Vol. 108, pp. 68-76.

Paduano, J., Valavani, L., Epstein, A.H., Greitzer, E.M., Guenette, G.R., 1990, "Modelling for Control of Rotating Stall," to be presented at 29th IEEE Conference on Decision and Control, IEEE Control System Society, Honolulu, HI.

Silkowski, P.D., 1990, "Aerodynamic Design of Moveable Inlet Guide Vanes for Active Control of Rotating Stall," M.S. Thesis, Department of Aeronautics and Astronautics, MIT.

Yonke, W.A., Landy, R.J., Stewart, J.F., 1987, "HIDEC Adaptive Engine Control System Flight Evaluation Results," ASME Paper 87-GT-257.

10